Ultrafast Hole- and Electron-Transfer Dynamics in CdS-Dibromofluorescein (DBF) Supersensitized Quantum Dot Solar Cell Materials

ARTICLE *in* JOURNAL OF PHYSICAL CHEMISTRY LETTERS · NOVEMBER 2013

Impact Factor: 7.46 · DOI: 10.1021/jz402315p

3 AUTHORS:

Partha Maity
Bhabha Atomic Research Centre
17 PUBLICATIONS **55** CITATIONS
SEE PROFILE

Tushar Debnath
Department of Atomic Energy
17 PUBLICATIONS **55** CITATIONS
SEE PROFILE

Hirendra N Ghosh
Bhabha Atomic Research Centre
127 PUBLICATIONS **3,859** CITATIONS
SEE PROFILE

THE JOURNAL OF PHYSICAL CHEMISTRY Letters

Letter

pubs.acs.org/JPCL

Ultrafast Hole- and Electron-Transfer Dynamics in CdS–Dibromofluorescein (DBF) Supersensitized Quantum Dot Solar Cell Materials

Partha Maity, Tushar Debnath, and Hirendra N. Ghosh*

Radiation and Photochemistry Division, Bhabha Atomic Research Centre, Mumbai 400085, India

Supporting Information

ABSTRACT: Ultrafast charge-transfer (CT) dynamics has been demonstrated in CdS quantum dot (QD)–4′,5′-dibromofluorescein (DBF) composite materials, which form a strong CT complex in the ground state. Charge separation in the CdS–DBF composite was found to take place in three different pathways, by transferring the photoexcited hole of CdS to DBF, electron injection from photoexcited DBF to the CdS QD, and direct electron transfer from the HOMO of DBF to the conduction band of the CdS QD. CT dynamics was monitored by direct detection of the DBF cation radical and electron in the QD in the transient absorption spectra. Electron injection and the electron-transfer process are found to be pulse-width-limited (<100 fs); however, the hole-transfer time was measured to be 800 fs. Charge recombination dynamics has been found to be very slow, confirming spatial charge separation in the CdS–DBF supersensitized quantum dot system. Grand charge separation process suggests that the CdS–DBF supersensitized quantum dot system can be used as superior materials for quantum dot solar cells (QDSCs).

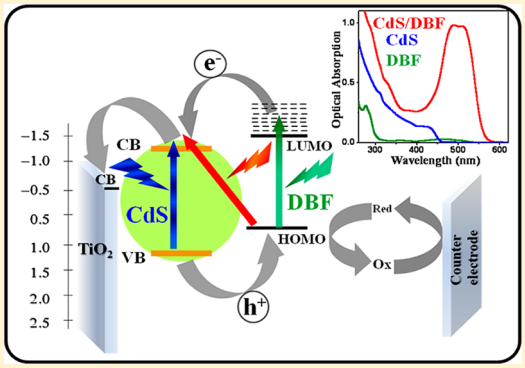

SECTION: Energy Conversion and Storage; Energy and Charge Transport

Charge transfer (CT) in quantum dot (QD)–molecular adsorbate composites is extremely important for their application in many electronic devices like QD-based solar cells.[1−5] In addition to that, interest of CT in molecule–QD systems has been increased manifold due to reports on multiple exciton generation (MEG) in QDs.[6−12] It has been realized and partially verified that the efficiency of solar modules can be enhanced significantly by dissociating or separating the multiexciton before ultrafast exciton–exciton annihilation.[13−15]

Using a suitable adsorbate molecule (electron or hole acceptors) on photoexcited QD materials, ultrafast exciton dissociation can be a reality. Exciton dissociation on fast and ultrafast time scales through electron transfer in QD–molecular adsorbate and QD–semiconductor nanoparticle (TiO_2) systems have been widely investigated.[3−5,16−18]

So far, the highest conversion efficiency in quantum dot solar cells (QDSCs) has been reported by Kamat and co-workers[19] to be ∼5.2%. However, by introducing an inorganic–organic heterojunction[20] and hybrid passivation,[21] the efficiency has been improved up to 7%, which is much lower than that of conventional dye-sensitized solar cells (DSSCs).[22] The main factors for overall lower efficiency are mainly due to limited absorption of solar radiation of the QD materials and a slow hole-transfer rate. Sizes of the QDs are higher (more than 2–3 nm, sometimes larger) as compared to dye molecules (the size is less than 1 nm), and as a result, QD loading on a TiO_2 electrode in the QDSC is much less as compared to dye loading in the DSSC. As a result, injected electrons in the QDSC are in direct contact with the electrolyte, which is undesirable. Finding a suitable hole-transporting material in QDSCs is always a challenging task. All of the problems can be tackled by introducing the concept of supersensitization in solar cells.[23−26] In supersensitization, the QD and molecular adsorbate can exchange charge carriers, where the molecular adsorbate, in addition to photosensitizing the QD material, also can act as a hole-transporting material, where holes are generated out of photoexcitation of the QD. As a result, grand charge separation can take place in the QD–molecular composite material, and it can be used as a supersensitizer. Lian[27] and Ghosh[28] and co-workers have observed in a dye–nanoparticles (TiO_2) system that charge separation facilitated drastically if the composite materials formed a CT complex in the ground state. Similarly, one can envisage charge separation between the QD and molecular adsorbate can be drastically improved if they form a CT complex in the ground state, where upon photoexcitation, an electron from the dye molecules can be transferred directly to the QD materials. To date, no report is available in the literature on CT complex formation in dye–QD composite systems nor on charge (both hole and electron) transfer dynamics on ultrafast time scales in such systems where the composite system can be used as a supersensitizer in QDSCs.

Received: October 27, 2013
Accepted: November 11, 2013
Published: November 11, 2013

Herein, we have chosen the CdS QD and dibromofluorescein (DBF) dye molecule to demonstrate grand charge separated state in supersensitized QDSCs, where both the CdS QD[23,24,26] and DBF[29,30] individually can sensitize TiO_2 nanoparticles. Redox energy levels of the CdS QD and DBF molecule imply that the conduction band (CB) of CdS lies below the LUMO level, which allows photoexcited DBF to inject an electron into the CB of the CdS QD and the HOMO level of DBF to lie above the valence band (VB) of the CdS QD (Supporting Information), allowing photoexcited hole transfer to the DBF molecule. Interestingly, the CdS QD and DBF forms a strong CT complex where upon photoexcitation, direct electron transfer from the DBF to CdS QD is feasible. We have carried out steady-state and time-resolved emission measurements to confirm hole- and electron-transfer processes following different pathways in the above system. Femtosecond transient absorption spectroscopy and fluorescence up-conversion techniques have been employed to monitor the charge (both electron and hole) transfer dynamics on an ultrafast time scale and to demonstrate grand charge separation in the CdS QD−DBF composite system.

Formation of a CT complex in the ground state between the molecular adsorbate and oxide semiconductor (TiO_2 and ZrO_2) is quite well-known in the literature.[31] In our earlier investigation, we also reported formation of a CT complex between the molecular adsorbate and TiO_2[28,32,33] and ZrO_2[32,33] nanoparticles, where appearance of a new CT optical absorption band was detected in the ground state. To the best of our knowledge, to date, no report is available where the QD (CdSe, CdS, CdTe, etc.) and molecular adsorbate form a CT complex in the ground state. Figure 1 shows the optical

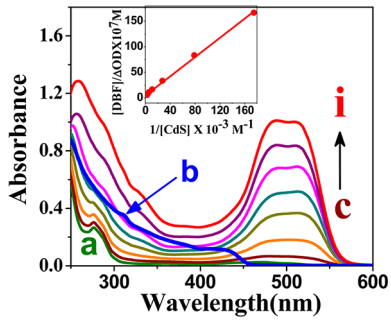

Figure 1. Optical absorption spectra of (a) DBF dye (0.3 mM), (b) CdS QD (0.49 μM), and (c−i) DBF−CdS complex at constant DBF concentration (0.3 mM) with increasing CdS QD concentration in chloroform (in the mixture, [CdS] are (c) 0.049, (d) 0.098, (e) 0.147, (f) 0.196, (g) 0.294, (h) 0.392, and (i) 0.49 μM). (Inset) Benesi−Hilderband (B−H) plot of the DBF−CdS CT complex.

absorption spectra of DBF after addition of different concentrations of CdS QDs. The pure DBF molecule shows weak optical absorption up to 550 nm with a peak at 465 in addition to an absorption band below 280 nm, as depicted in trace a in Figure 1. The CdS QDs (spherical in size) were synthesized adopting a high-temperature injection method[34] (synthesis of the CdS QD and HRTEM image are shown in the Supporting Information).

Trace b in Figure 1 depicts the optical absorption spectrum of the 0.49 μM CdS QD in chloroform, which shows an exciton at 433 nm, and the corresponding band gap can be calculated to be ~2.69 eV. Now, upon addition of increasing concentrations (0.049−0.49 μM) of CdS QDs in DBF solution, the optical absorption band becomes broader and shifted to the red region of the spectrum. The color of the solution becomes deep red (while the colors of free DBF and CdS are light orange and yellow, respectively), indicating formation of a strong CT complex between the CdS QD and DBF. The intensity of the CT band increases drastically. A Benesi−Hilderband (BH) plot for the above CdS−DBF system is shown in the inset of Figure 1, where the extinction coefficient of the complex is calculated to be 2.14×10^6 M^{-1} cm^{-1}. A high extinction coefficient of the CdS−DBF complex suggests that the composite materials form a strong CT complex where partial charge transfer takes place in the ground state. This observation clearly suggests that the CdS−DBF composite material is a potential material for a supersensitizer, which can absorb more solar radiation as compared to that of the individual CdS QD and DBF molecule.

Trace a in Figure 2 shows steady-state luminescence spectra of the CdS QD in chloroform after exciting the sample at 375

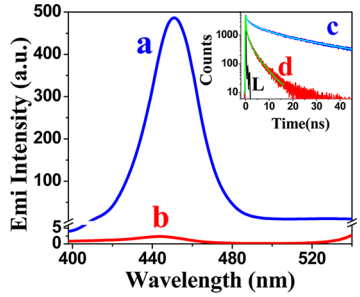

Figure 2. Photoluminescence (PL) spectra of the CdS QD (a) in the absence and (b) in the presence of DBF in a chloroform solution after exciting at 375 nm. (Inset) Emission decay traces of the (c) CdS QD and (d) CdS−DBF composite after exciting at 406 nm and monitoring at 450 nm. **L** is the excitation profile. [CdS] = 0.49 μM and [DBF] = 0.3 mM.

nm, which consists if an emission peak at 450 nm with a high quantum yield (φ_f = 0.24). Trace b in Figure 2 shows the emission spectra of the CdS QD in the presence of 0.3 mM DBF. It is clearly seen that CdS emission is completely quenched in the presence of DBF. As we have already mentioned that the VB (1.35 V versus NHE) of CdS lies below the HOMO (0.8 V vs NHE) of DBF (Scheme 1), the photoexcited hole can be captured by DBF, which is thermodynamically viable. The hole-transfer reaction can be expressed by the equations below:

$$CdS + h\nu \rightarrow CdS(e^- + h^+) \quad (1)$$

$$CdS(e^- + h^+) + DBF \rightarrow CdS(e^-) + DBF^+ \quad (2)$$

To find the hole-transfer dynamics, we have carried out time-resolved emission studies of free CdS QDs and also in the presence of DBF, shown in the Figure 2 inset. The emission decay traces of the CdS QD and CdS−DBF composite have been monitored at 450 nm after exciting the samples at 406 nm. The emission decay traces can be fitted multiexponentially with time constants of τ_1 = 0.58 ns (39%), τ_2 = 23.8 ns (32%), and τ_3 = 5.2 ns (29%) with τ_{avg} = 9.4 ns for the CdS QD and of τ_1 = 0.12 ns (61%), τ_2 = 0.94 ns (22%), and τ_3 = 3.4 ns (17%) with τ_{avg} = 0.9 ns for the CdS−DBF system. The average lifetime of the CdS−DBF system is 10 times shorter as compared to that of the CdS QD, which confirms a hole-transfer process in the composite materials, as suggested in eq 2. Presumably, the observed decrease in lifetime arises due to hole transfer (HT)

dx.doi.org/10.1021/jz402315p | J. Phys. Chem. Lett. 2013, 4, 4020−4025

Scheme 1. CT Processes (Hole Transfer, Electron Injection, and Charge Recombination Reactions) Involving CdS QDs and DBF Dye in Chloroform[a]

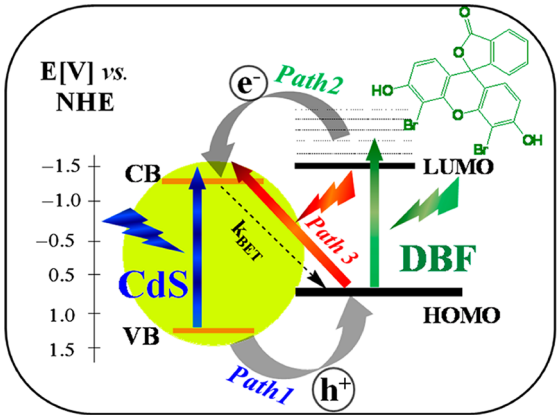

[a]The molecular structure of DBF is shown in the scheme.

from the CdS QD to DBF molecule, and then, the hole-transfer rate constant can be determined through the following expression

$$k_{HT} = \frac{1}{\tau_{CdS+DBF}} - \frac{1}{\tau_{CdS}} \quad (3)$$

Using the average lifetime values of 9.4 (CdS) and 0.9 ns (CdS−DBF), the hole-transfer rate constant can be determined to be 1.1×10^9 s^{-1}.

Now, from Scheme 1, it is clear that a photoexcited DBF molecule can inject an electron into the CB of the CdS QD. To monitor this electron-transfer process from a photoexcited DBF to CdS QD, we have carried out emission spectroscopy in the present investigation after exciting the DBF molecule. Electron injection dynamics from photoexcited xanthenes dyes (DBF is a xanthenes dye) to the CB of TiO_2 have been demonstrated by us.[33] Because xanthenes dye molecules are highly luminescent, it is easy to demonstrate the electron-transfer process by monitoring the luminescence quenching measurements.

Figure 3 depicts the emission spectra of DBF and the DBF−CdS composite after exciting the samples at 500 nm. Trace a in Figure 3 shows the emission spectrum of DBF, which has an emission peak at 557 nm with a hump at 584 nm. However, in the presence of CdS, the emission intensity drastically reduces,

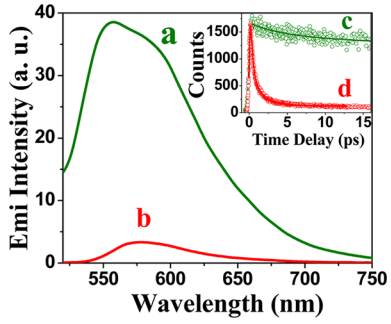

Figure 3. PL spectra of DBF (a) in the absence and (b) in the presence of a CdS QD after exciting at 500 nm. (Inset) Fluorescence up-conversion traces of (c) DBF and (d) the CdS−DBF composite after exciting at 435 nm and monitoring at 560 nm in chloroform. [CdS] = 0.49 μM and [DBF] = 0.3 mM.

as shown in trace b in Figure 3. Again, as we have already mentioned that the LUMO (−1.5 V) of DBF lies above the CB (−1.3 V versus NHE) of the CdS QD (Scheme 1), photoexcited DBF can inject an electron into the CB of CdS. The emission quenching can be attributed to electron injection from photoexcited DBF to CdS and can be expressed by the equations below:

$$DBF + h\nu \rightarrow DBF^* \quad (4)$$

$$DBF^* + CdS\ QD \rightarrow DBF^+ + CdS\ QD(e^-) \quad (5)$$

Now, to monitor electron injection dynamics, we have carried out fluorescence up-conversion measurements for free DBF and also in the presence of a CdS QD after exciting the samples with a 435 nm laser pulse and monitoring at 560 nm, shown in the Figure 3 inset. We would like to make a point that by exciting pure CdS at 435 and monitoring at 560 nm, no emission signal was observed. It is clear from the emission decay trace of pure DBF (Figure 3c) that the emission lifetime of DBF is too long to be measured by the fluorescence up-conversion technique. Therefore, to measure the emission lifetime of DBF, we performed nanosecond lifetime measurements (TCSPC) and determined it to be 1.6 ns (Supporting Information). Trace d in Figure 3 depicts the emission kinetics of DBF in the presence of a CdS QD, which can be fitted biexponentially with time constants of τ_1 = 618 fs (85%) and τ_2 = 1.8 ps (15%) with average lifetime τ_{avg} = 800 fs. If we presume that the observed decrease in lifetime arises due to electron injection from photoexcited DBF to the CdS QD, then we can determine the electron injection time constant by the following expression:

$$k_{inj} = \frac{1}{\tau_{DBF+CdS}} - \frac{1}{\tau_{DBF}} \quad (6)$$

By following the above expression, the electron injection rate can be determined to be 1.2×10^{12} s^{-1}. With the help of the time-resolved emission technique, we have demonstrated both electron injection from photoexcited DBF to the CdS QD and also hole transfer from the photoexcited CdS QD to DBF molecule.

To corroborate charge (both electron and hole) transfer dynamics on an early time scale with more accuracy, we have carried out femtosecond transient absorption spectroscopic measurements by exciting CdS QD, DBF, and DBF−CdS QD composite systems at 400 nm laser light. Figure 4 shows the transient absorption spectra of photoexcited CdS−DBF QD composite materials at different time delays, which comprises a

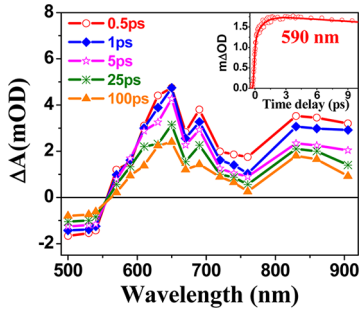

Figure 4. Transient absorption spectra of CdS−DBF composite materials in chloroform at different time delays after excitation with 400 nm laser light. (Inset) Kinetic decay trace at 590 nm.

dx.doi.org/10.1021/jz402315p | J. Phys. Chem. Lett. 2013, 4, 4020−4025

bleach below 550 nm and two broad absorption bands at 550−750 and 750−900 nm, respectively. The broad spectral absorption in the 750−900 nm region can be attributed to the electrons in the CB in the CdS QD. The transient absorption band at 550−750 nm can be attributed to the DBF cation radical. The band having a maximum at 650 nm is assigned to the DBF cation radical ($DBF^{\bullet+}$). Assignment of this band has been made on the basis of the results obtained in separate pulse radiolysis experiments (Supporting Information), where $DBF^{\bullet+}$ was generated selectively by the reaction of a $N_3^{\bullet}$ radical with a DBF molecule in a N_2O-saturated aqueous solution. We have already demonstrated that at 400 nm photoexcitation, both electron injection and a hole-transfer process can occur in DBF−CdS composite materials. Now, to understand the CT dynamics, we have monitored the kinetics at 500 (bleach wavelength), 650 (DBF cation radical), and 900 nm (electron in QD), shown in Figure 5. The bleach recovery

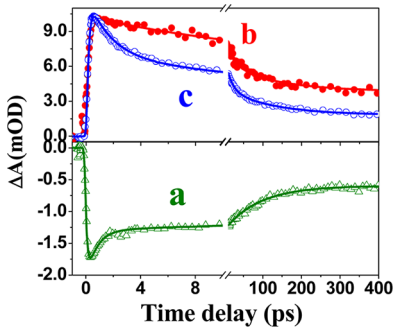

Figure 5. Kinetic decay traces at (a) 500, (b) 650, and (c) 900 nm for the CdS−DBF system in chloroform after exciting the samples at 400 nm laser light.

kinetics at 500 nm (trace a in Figure 5) can be fitted with time constants of τ_1 = 800 fs (25%), τ_2 = 90 ps (37%), and τ_3 > 400 ps (38%). The transient signal due to the cation radical of DBF at 650 nm can be fitted multiexponentially with a growth of ∼350 fs and decay components of τ_1 = 15 ps (47%), τ_2 = 90 ps (13%), and τ_3 > 400 ps (40%). Interestingly, the transient signal decay due to an electron in the CdS QD can be fitted multiexponentially with time constants of τ_1 = 1.2 ps (40%), τ_2 = 15 ps (27%), τ_3 = 90 ps (12%), and τ_4 > 400 ps (21%). Although the transient peak at 650 nm indicates the peak of the DBF cation radical, the contribution due to an electron at 650 nm cannot be ignored. Therefore, to observe the kinetics for the cation radical, we have also monitored the growth signal at 590 nm, which can be fitted biexponentially with τ_1 = ∼100 fs (61%) and τ_2 = 800 fs (39%) and is shown in the Figure 4 inset. In our earlier studies,[33] we have observed in dye-sensitized TiO_2 nanoparticle systems that the growth kinetics for both the injected electron and oxidized dye cation radical are similar, which indicates that charge separation takes place through one process only, that is, through electron injection from the photoexcited state to CB of TiO_2. However, in the present investigation, we have observed that growth and decay kinetics for the DBF cation radical at 590 nm is different from that of the electron at 900 nm. This observation clearly suggests that generation of an electron in the CB in CdS and formation of the DBF cation radical might be taking place through more than one process and has been discussed in the next section.

Recent investigation on QDSCs suggests that removal of charges (holes and electrons) from photoexcited QDs can be a key factor to improve the conversion efficiency. In CdS−DBF composite materials, it is clear from Scheme 1 that DBF can extract the photoexcited hole from the CdS QD (path 1, Scheme 1). In addition to that, photoexcited DBF can inject an electron to the CB of CdS (path 2, Scheme 1), suggesting that CdS−DBF is a typical type II system of the QD−molecular system. Over and above the formation of a type II system, from steady-state optical absorption measurements (Figure 1), it is clear that the CdS QD and DBF form a strong CT complex with a very high molecular extinction coefficient, which has an absorption band in the red region of the solar radiation as compared to both the CdS QD and DBF molecule; as a result, the absorption cross section of the CdS−DBF composite system toward solar radiation increases dramatically. Upon excitation of the CT CdS−DBF complex, the electron from the HOMO of DBF can move directly to the CB of CdS (path 3, Scheme 1), which ensures much higher charge separation as compared to both hole transfer from CdS to DBF and also electron injection from photoexcited DBF to the CB of CdS. We have demonstrated that the blue, green, and red parts of the solar radiation will be absorbed by the CdS QD, DBF, and CdS−DBF CT complex, respectively, as shown in Scheme 1. Now, it is very important to unravel the CT dynamics in the CdS−DBF composite system as excited by 400 nm femtosecond laser pulse. We have already mentioned that the absorption cross section of pure DBF is very poor; however, both the CdS QD and CdS−DBF complex can absorb 400 nm light quite effectively. We have observed that the growth kinetics for the DBF cation radical at 590 nm can be fitted biexponentially with time constants of ∼100 (61%) and 800 fs (39%). The fast growth component (<100 fs) can be attributed to direct electron transfer upon excitation of the CT complex (path 3, Scheme 1); on the other hand, the 800 fs component can be attributed to photoexcited hole transfer from the VB of CdS to DBF (path 1, Scheme 1). To the best of our knowledge this is one of the first reports on hole-transfer dynamics on the ultrafast time scale in supersensitized QDSCs. It is interesting to see that unlike the slower and biexponential appearance time for the DBF cation, we have observed a single-exponential and pulse-width-limited (<100 fs) appearance time for the electron in CdS. Excitation of CdS and direct excitation of the CdS−DBF complex populates an electron in the CB of CdS. As a result, we have observed a pulse-width-limited growth time for the appearance of electron signal. Now, let us discuss charge recombination dynamics in CdS−DBF composite materials. To monitor charge recombination dynamics, one can either monitor the bleach recovery kinetics at 500 nm or transient decay kinetics at 650 nm for the DBF cation radical or at 900 nm for the electron in the CdS QD. However, it is interesting to see that the dynamics are quite different, where it expected that the dynamics should be similar as it demonstrates same charge recombination reaction. Comparing the dynamics of 650 and 900 nm, it is seen that an extra fast component (1.2 ps) exists at 900 nm (Table 1). This extra fast component can be attributed to trapping dynamics of the electron in CdS QD, where some surface state exists in the QD material. On the other hand, at bleach recovery kinetics at 500 nm, we have observed 800 fs fast bleach recovery components, which might be due to a hole-transfer process as at this wavelength, there is a good overlap for both the ground-state bleach and DBF cation radical. Therefore, the kinetics at 650 nm can be attributed to charge recombination dynamics.

dx.doi.org/10.1021/jz402315p | J. Phys. Chem. Lett. 2013, 4, 4020−4025

Table 1. Lifetimes of the Transients for the CdS−DBF Composite System at Different Wavelengths

wavelength (nm)	τ_{growth}	τ_1 (%)	τ_2 (%)	τ_3 (%)	τ_4 (%)
500	<100 fs	800 fs (25%)	90 ps (37%)	>400 ps (38%)	
650	<350 fs	15 ps (47%)	90 ps (13%)	>400 ps (40%)	
905	<150 fs	1.2 ps (40%)	15 ps (27%)	90 ps (12%)	>400 ps (21%)

In the present studies steady state and time-resolved transient absorption and luminescence data confirm higher charge separation through supersensitization. The CdS−DBF composite not only effectively removes the hole from the QD, it can also absorbs more solar radiation due to formation of a CT complex that has a very high molar extinction coefficient. Considering the fact that QDSC photoaction is the exclusive outcome of kinetic competitions of electron injection, hole-transfer, back-electron-transfer, and dye regeneration processes, this supersensitization scheme can bring significant improvement in QDSCs without changing the device fabrication much.

In conclusion, ultrafast hole- and electron-transfer dynamics in the CdS QD−DBF composite are explored and verified as a supersensitizer in QDSCs. Optical absorption studies indicate that the CdS QD and DBF form a strong CT complex in the ground state. Steady-state and time-resolved absorption and emission studies confirmed that upon photoexcitation, charge separation in the CdS−DBF composite takes place via three different pathways, through hole transfer from the photoexcited CdS QD to DBF (path 1), electron injection from photoexcited DBF to the CdS QD (path 2), and finally, direct electron transfer from the ground-state (HOMO) DBF to the CB of the QD (path 3) (photoexcitation of the CT complex). As a result, grand charge separation takes place in the CdS−DBF composite, which confirms the usefulness as a supersensitizer in QDSCs. Ultrafast transient absorption and femtosecond up-conversion studies indicate that paths 2 and 3 are pulse-width-limited (<100 fs); however, the path 1 time was measured to be 800 fs. Charge recombination dynamics found were very slow due to spatial charge separation in the composite. This observation confirms the reality of multiple exciton dissociation and finally higher photoconversion efficiency in QDSCs.

■ ASSOCIATED CONTENT

Supporting Information

Details about the synthesis, high-resolution TEM images, cyclic voltametric measurements and ultrafast transient spectroscopy of the CdS QD and DBF, emission lifetime of DBF, pulse radiolytic studies of DBF, and the experimental setup for time-resolved up-conversion and transient absorption. This material is available free of charge via the Internet at http://pubs.acs.org.

■ AUTHOR INFORMATION

Corresponding Author

*E-mail: hnghosh@barc.gov.in. Fax: (+) 91-22-25505331/25505151.

Notes

The authors declare no competing financial interest.

■ ACKNOWLEDGMENTS

We thank Dr. Shilpa Tawade Chemistry Division, BARC, for her assistance with cyclic voltammetric measurements. P.M. acknowledges DAE and T.D. acknowledges CSIR for research fellowships. We also acknowledge Prof. Anindya Dutta, Department of Chemistry, IIT Mumbai for providing fluorescence up-conversion. We sincerely thank Dr. D. K. Palit and Dr. B. N. Jagatap for their encouragement.

■ REFERENCES

(1) Robel, I.; Subramanian, V.; Kuno, M.; Kamat, P. V. Quantum Dot Solar Cells. Harvesting Light Energy with CdSe Nanocrystals Molecularly Linked to Mesoscopic TiO_2 Films. *J. Am. Chem. Soc.* **2006**, *128*, 2385−2393.

(2) Kamat, P. V. Quantum Dot Solar Cells. The Next Big Thing in Photovoltaics. *J. Phys. Chem. Lett.* **2013**, *4*, 908−918.

(3) Morris-Cohen, A. J.; Frederick, M. T.; Cass, L. C.; Weiss, E. A. Simultaneous Determination of the Adsorption Constant and the Photoinduced Electron Transfer Rate for a CdS Quantum Dot−Viologen Complex. *J. Am. Chem. Soc.* **2011**, *133*, 10146−10154.

(4) Song, N.; Zhu, H.; Jin, S.; Lian, T. Hole Transfer from Single Quantum Dots. *ACS Nano* **2011**, *5*, 8750−8759.

(5) Huang, J.; Huang, Z.; Yang, Y.; Zhu, H.; Lian, T. Multiple Exciton Dissociation in CdSe Quantum Dots by Ultrafast Electron Transfer to Adsorbed Methylene Blue. *J. Am. Chem. Soc.* **2010**, *132*, 4858−4864.

(6) Schaller, R. D.; Klimov, V. I. High Efficiency Carrier Multiplication in PbSe Nanocrystals: Implications for Solar Energy Conversion. *Phys. Rev. Lett.* **2004**, *92*, 186601.

(7) Ellingson, R. J.; Beard, M. C.; Johnson, J. C.; Yu, P.; Micic, O. I.; Nozik, A. J.; Shabaev, A.; Efros, A. L. Highly Efficient Multiple Exciton Generation in Colloidal PbSe and PbS Quantum Dots. *Nano Lett.* **2005**, *5*, 865−871.

(8) Luther, J. M.; Beard, M. C.; Song, Q.; Law, M.; Ellingson, R. J.; Nozik, A. J. Multiple Exciton Generation in Films of Electronically Coupled PbSe Quantum Dots. *Nano Lett.* **2007**, *7*, 1779−1784.

(9) Schaller, R. D.; Sykora, M.; Pietryga, J. M.; Klimov, V. I. Seven Excitons at a Cost of One: Redefining the Limits for Conversion Efficiency of Photons into Charge Carriers. *Nano Lett.* **2006**, *6*, 424−429.

(10) Murphy, J. E.; Beard, M. C.; Norman, A. G.; Ahrenkiel, S. P.; Johnson, J. C.; Yu, P.; Micic, O. I.; Ellingson, R. J.; Nozik, A. J. PbTe Colloidal Nanocrystals: Synthesis, Characterization, and Multiple Exciton Generation. *J. Am. Chem. Soc.* **2006**, *128*, 3241−3247.

(11) Stewart, J. T.; Padilha, L. A.; Bae, W. K.; Koh, W.-K.; Pietryga, J. M.; Klimov, V. I. Carrier Multiplication in Quantum Dots within the Framework of Two Competing Energy Relaxation Mechanisms. *J. Phys. Chem. Lett.* **2013**, *4*, 2061−2068.

(12) Schaller, R. D.; Pietryga, J. M.; Klimov, V. I. Carrier Multiplication in InAs Nanocrystal Quantum Dots with an Onset Defined by the Energy Conservation Limit. *Nano Lett.* **2007**, *7*, 3469−3476.

(13) Klimov, V. I. Spectral and Dynamical Properties of Multiexcitons in Semiconductor Nanocrystals. *Annu. Rev. Phys. Chem.* **2007**, *58*, 635−673.

(14) Nozik, A. J. Spectroscopy and Hot Hole Relaxation Dynamics in Semiconductor Quantum Wells and Quantum Dots. *Annu. Rev. Phys. Chem.* **2001**, *52*, 193−231.

(15) Beard, M. C.; Luther, J. M.; Semonin, O. E.; Nozik, A. J. Third Generation Photovoltaics based on Multiple Exciton Generation in Quantum Confined Semiconductors. *Acc. Chem. Res.* **2013**, *46*, 1252−1260.

(16) Tisdale, W. A.; Williams, K. J.; Timp, B. A.; Norris, D. J.; Aydil, E. S.; Zhu, X.-Y. Hot-Electron Transfer from Semiconductor Nanocrystals. *Science* **2010**, *328*, 1543−1547.

(17) Yang, Y.; Rodríguez-Córdoba, W.; Xiang, X.; Lian, T. Strong Electronic Coupling and Ultrafast Electron Transfer between PbS Quantum Dots and TiO_2 Nanocrystalline Films. *Nano Lett.* **2012**, *12*, 303−309.

(18) Robel, I.; Kuno, M.; Kamat, P. V. Size-Dependent Electron Injection from Excited CdSe Quantum Dots into TiO_2 Nanoparticles. *J. Am. Chem. Soc.* **2007**, *129*, 4136−4137.

(19) Santra, P. K.; Kamat, P. V. Mn-Doped Quantum Dot Sensitized Solar Cells: A Strategy to Boost Efficiency over 5%. *J. Am. Chem. Soc.* **2012**, *134*, 2508−2511.
(20) Chang, J. A.; Im, S. H.; Lee, Y. H.; Kim, H.-j.; Lim, C.-S.; Heo, J. H.; Seok, S. I. Panchromatic Photon-Harvesting by Hole-Conducting Materials in Inorganic−Organic Heterojunction Sensitized-Solar Cell through the Formation of Nanostructured Electron Channels. *Nano Lett.* **2012**, *12*, 1863−1867.
(21) Ip, A. H.; Thon, S. M.; Hoogland, S.; Voznyy, O.; Zhitomirsky, D.; Debnath, R.; Levina, L.; Rollny, L. R.; Carey, G. H.; Fischer, A.; Kemp, K. W.; Kramer, I. J.; Ning, Z.; Labelle, A. J.; Chou, K. W.; Amassian, A.; Sargent, E. H. Hybrid Passivated Colloidal Quantum Dot Solids. *Nat. Nanotechnol.* **2012**, *7*, 577−582.
(22) Yella, A.; Lee, H.-W.; Tsao, H. N.; Yi, C.; Chandiran, A. K.; Nazeeruddin, M. K.; Diau, E.W.-G.; Yeh, C.-Y.; Zakeeruddin, S. M.; Grätzel, M. Porphyrin-Sensitized Solar Cells With Cobalt (II/III)-Based Redox Electrolyte Exceed 12% Efficiency. *Science* **2011**, *334*, 629−634.
(23) Lee, H. J.; Leventis, H. C.; Moon, S.-J.; Chen, P.; Ito, S.; Haque, S. A.; Torres, T.; Nüesch, F.; Geiger, T.; Zakeeruddin, S. M.; Grätzel, M.; Nazeeruddin, M. K. PbS and CdS Quantum Dot-Sensitized Solid-State Solar Cells: "Old Concepts, New Results". *Adv. Funct. Mater.* **2009**, *19*, 2735−2742.
(24) Choi, H.; Nicolaescu, R.; Paek, S.; Ko, J.; Kamat, P. V. Supersensitization of CdS Quantum Dots with NIR Organic Dye: Towards the Design of Panchromatic Hybrid-Sensitized Solar Cells. *ACS Nano* **2011**, *5*, 9238−9245.
(25) Shalom, M.; Albero, J.; Tachan, Z.; Martínez-Ferrero, E.; Zaban, A.; Palomares, E. Quantum Dot-Dye Bilayer-Sensitized Solar Cells: Breaking the Limits Imposed by the Low Absorbance. *J. Phys. Chem. Lett.* **2010**, *1*, 1134−1138.
(26) Mora-Sero, I.; Bisquert, J. Breakthroughs in the Development of Semiconductor-Sensitized Solar Cells. *J. Phys. Chem. Lett.* **2010**, *1*, 3046−3052.
(27) Wang, Y.; Hang, K.; Anderson, N. A.; Lian, T. Comparison of Electron Transfer Dynamics in Molecule-to-Nanoparticle and Intramolecular Charge Transfer Complexes. *J. Phys. Chem. B* **2003**, *107*, 9434−9440.
(28) Ramakrishna, G.; Ghosh, H. N.; Singh, A. K.; Palit, D. K.; Mittal, J. P. Dynamics of Back Electron Transfer Processes of Strongly Coupled Triphenyl Methane Dyes Adsorbed on TiO_2 Nanoparticle Surface as Studied by Fast and Ultrafast Visible Spectroscopy. *J. Phys. Chem. B.* **2001**, *105*, 12786−12796.
(29) Ramakrishna, G.; Ghosh, H. N. Emission from the Charge Transfer State of Xanthene Dye-Sensitized TiO_2 Nanoparticles: A New Approach to Determining Back Electron Transfer Rate and Verifying the Marcus Inverted Regime. *J. Phys. Chem. B* **2001**, *105*, 7000−7008.
(30) Ramakrishna, G.; Das, A.; Ghosh, H. N. Effect of Surface Modification on Back Electron Transfer of Dibromo Fluorescein (DBF) Sensitized TiO_2 Nanoparticles. *Langmuir* **2004**, *20*, 1430−1435.
(31) Rajh, T.; Chen, L. X.; Lukas, K.; Liu, T.; Thurnauer, M. C.; Teide, D. M. Surface Restructuring of Nanoparticles: An Efficient Route for Ligand−Metal Oxide Crosstalk. *J. Phys. Chem. B* **2002**, *106*, 10543−10552.
(32) Ramakrishna, G.; Singh, A. K.; Palit, D. K.; Ghosh, H. N. Dynamics of Interfacial Electron Transfer from Photoexcited Quinizarin (Qz) into the Conduction Band of TiO_2 and Surface States of ZrO_2 Nanoparticles. *J. Phys. Chem. B* **2004**, *108*, 4775−4783.
(33) Maity, P.; Debnath, T.; Akbar, A.; Verma, S.; Ghosh, H. N. Ultrafast Electron Transfer and Trapping Dynamics in the Inter-Band-Gap States of ZrO_2 Nanoparticles Sensitized by Baicalein (BIC). *J. Phys. Chem. C* **2013**, *117*, 17531−17539.
(34) Yu, W. W.; Qu, L.; Guo, W.; Peng, Xi. Experimental Determination of the Extinction Coefficient of CdTe, CdSe, and CdS Nanocrystals. *Chem. Mater.* **2003**, *15*, 2854−2860.